

# Linking Anthropogenic Chlorine Emissions to Regional Air Quality in India

Ankit Patel<sup>1,2\*</sup>, Malasani Chakradhar Reddy<sup>1,2</sup>, Bingqing Zhang<sup>3</sup>, Basudev Swain<sup>4</sup>,  
Govindan Pandithurai<sup>1</sup>, Meinrat O. Andreae<sup>5,6</sup>, Scot T. Martin<sup>7,8</sup>, Pengfei Liu<sup>3</sup>,  
Sachin S. Gunthe<sup>1,2\*</sup>

<sup>1</sup>Centre for Atmospheric and Climate Sciences, Indian Institute of Technology Madras,  
Chennai-600 036, India.

<sup>2</sup>Environmental Engineering Division, Department of Civil Engineering, Indian Institute of  
Technology Madras, Chennai-600 036, India.

<sup>3</sup>School of Earth and Atmospheric Sciences, Georgia Institute of Technology, Atlanta,  
Georgia 30332, United States.

<sup>4</sup>Atmospheric, Oceanic and Planetary Physics, University of Oxford, Oxford, United  
Kingdom.

<sup>5</sup>Multiphase Chemistry Department, Max Planck Institute for Chemistry, Mainz 55128,  
Germany.

<sup>6</sup>Scripps Institution of Oceanography, University of California, San Diego, La Jolla,  
California 92093, United States.

<sup>7</sup>Department of Earth and Planetary Sciences, Harvard University, Cambridge,  
Massachusetts 02138, United States.

<sup>8</sup>John A. Paulson School of Engineering and Applied Sciences, Harvard University,  
Cambridge, Massachusetts 02138, United States.

\*Corresponding author(s). E-mail(s): [ankitpatel0698@cacs.iitm.ac.in](mailto:ankitpatel0698@cacs.iitm.ac.in); [s.gunthe@iitm.ac.in](mailto:s.gunthe@iitm.ac.in);

# Supplementary Material

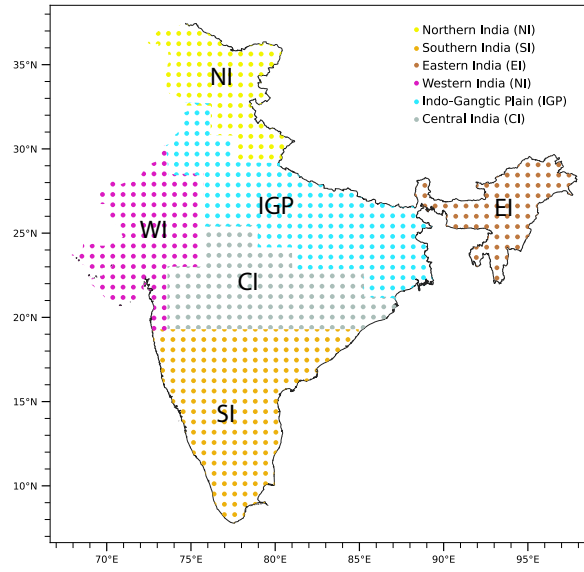


Fig. 1 Indian region divided into six different regions based on different geographical and topographical features [1]

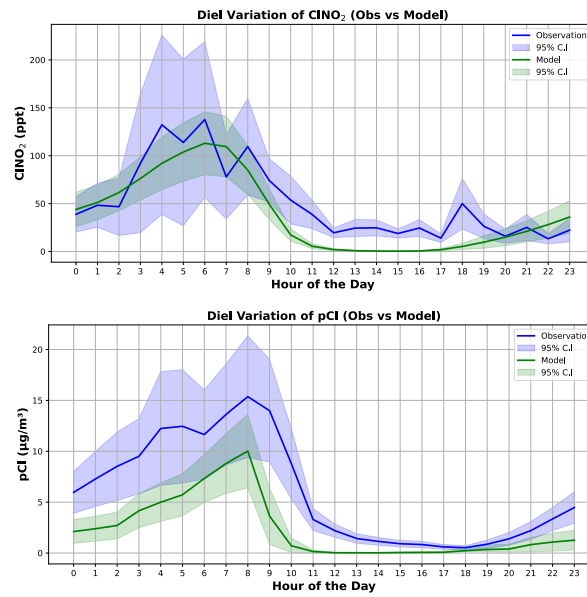
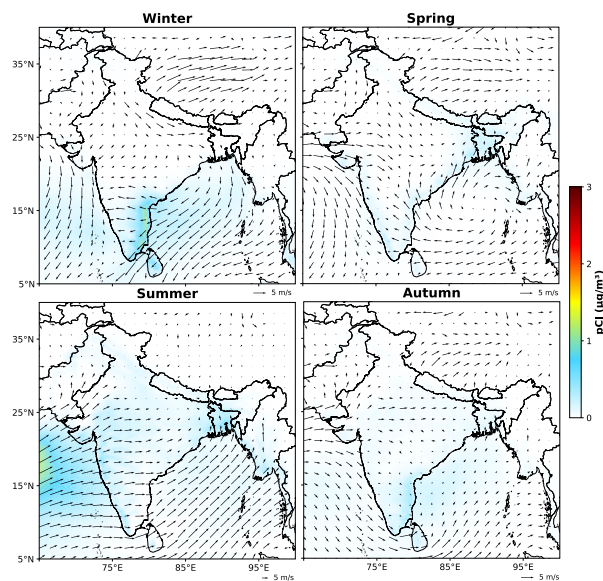
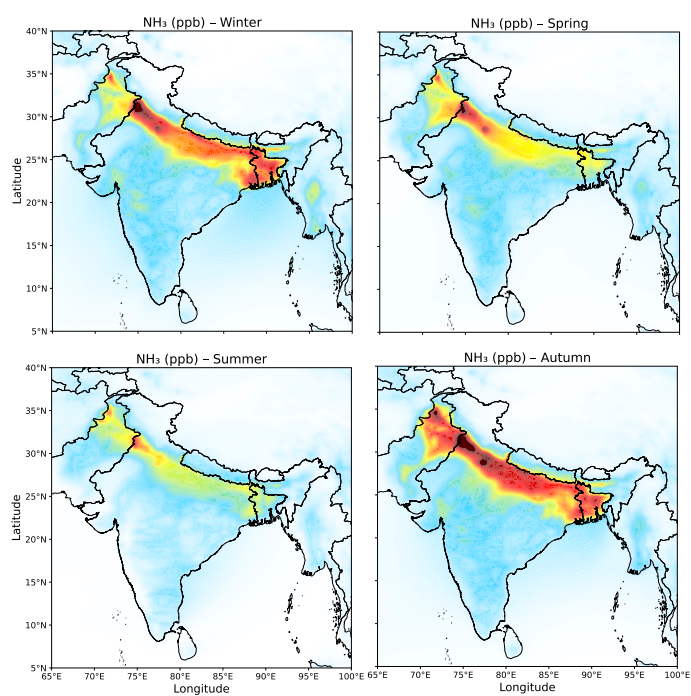


Fig. 2 Model vs Observation of diel variation of ClNO<sub>2</sub> and pCl<sup>-</sup> at New Delhi, India. Observation data of ClNO<sub>2</sub> is taken for January-February 2019 [2] and pCl<sup>-</sup> is for February-March from [3].





**Fig. 3** Seasonal distribution of modelled  $\text{pCl}^-$  concentrations ( $\mu\text{g m}^{-3}$ ) from the Wo-AnthroHCl simulation, shown together with wind patterns. The results highlight the influence of marine transport on coastal regions across all seasons.



**Fig. 4** Seasonal spatial distribution of  $\text{NH}_3$  (ppb) from the Wi-AnthroHCl simulation over the Indian subcontinent.

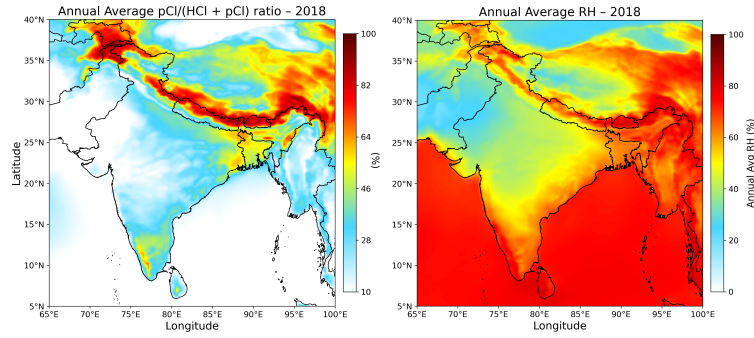


**Fig. 5** Spatial distribution of Annual average relative humidity (%) and the  $pCl^-$  partitioning ratio efficiency ( $pCl^- / HCl + pCl^-$ ) for 2018.

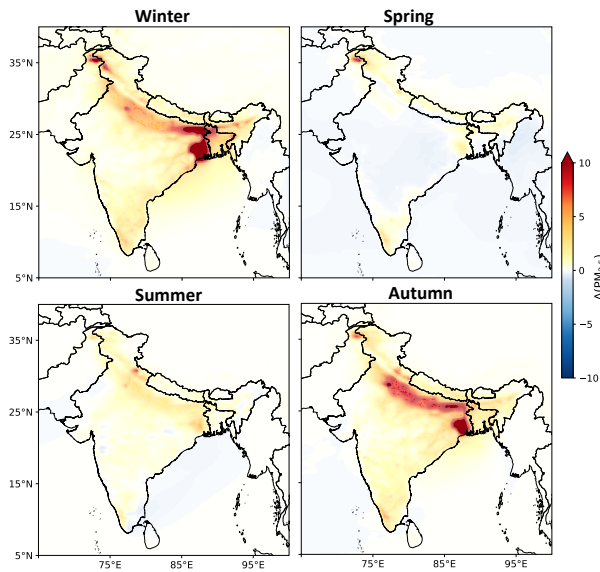


**Fig. 6** Spatial distribution of  $\Delta PM_{2.5}$  for each season calculated as the difference between Wi-AnthroHCl and Wo-AnthroHCl simulation

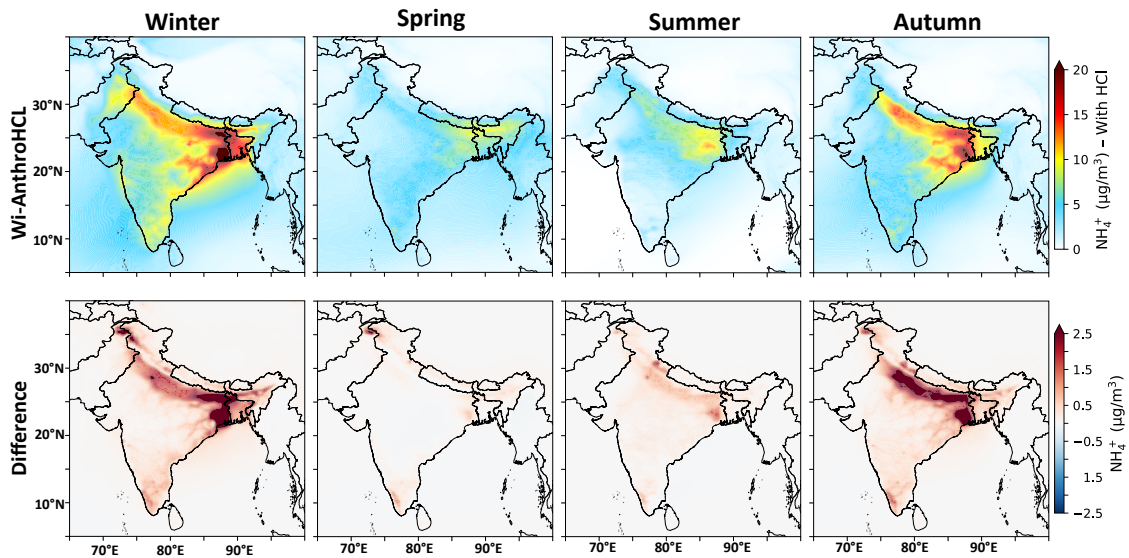


**Fig. 7** Spatial distribution of  $NH_4^+$  from Wi-AnthroHCl simulation and the absolute difference between Wi-AnthroHCl and Wo-AnthroHCl simulations for each season

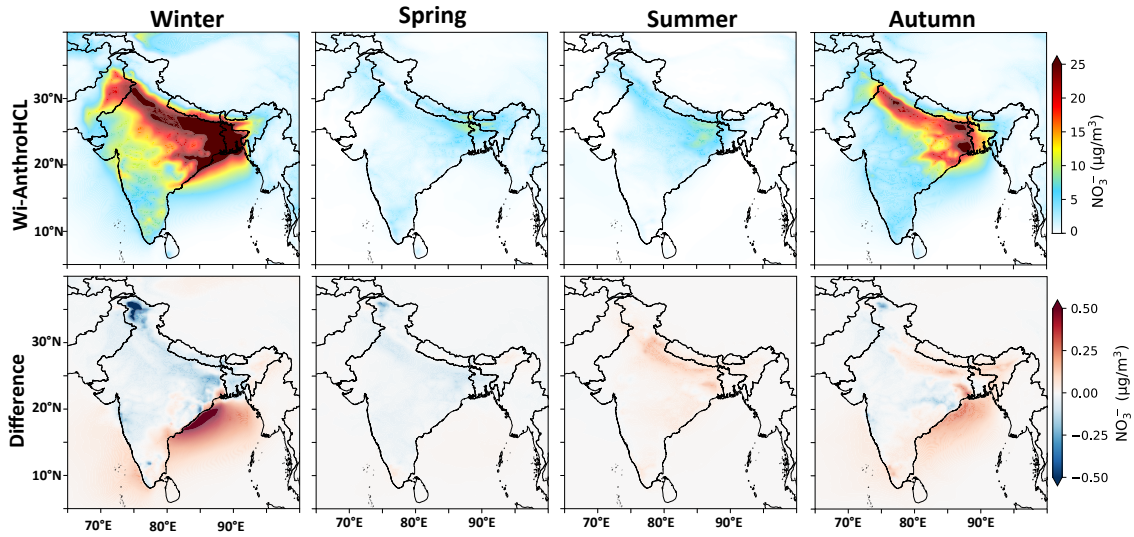


**Fig. 8** Spatial distribution of  $\text{NO}_3^-$  from Wi-AnthroHCl simulation and the absolute difference between Wi-AnthroHCl and Wo-AnthroHCl simulations for each season

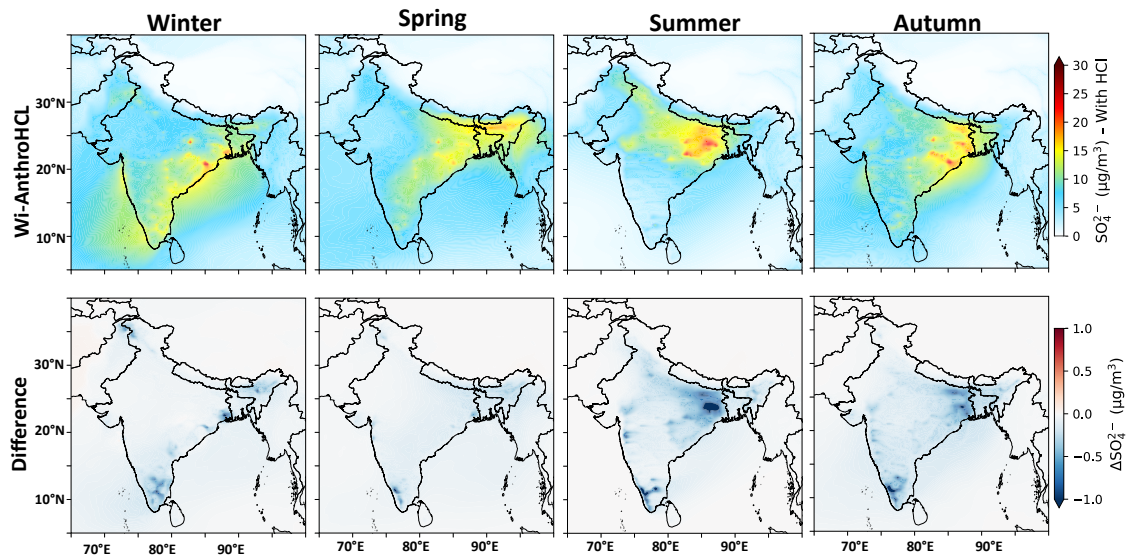


**Fig. 9** Spatial distribution of  $\text{SO}_4^{2-}$  from Wi-AnthroHCl simulation and the absolute difference between Wi-AnthroHCl and Wo-AnthroHCl simulations for each season

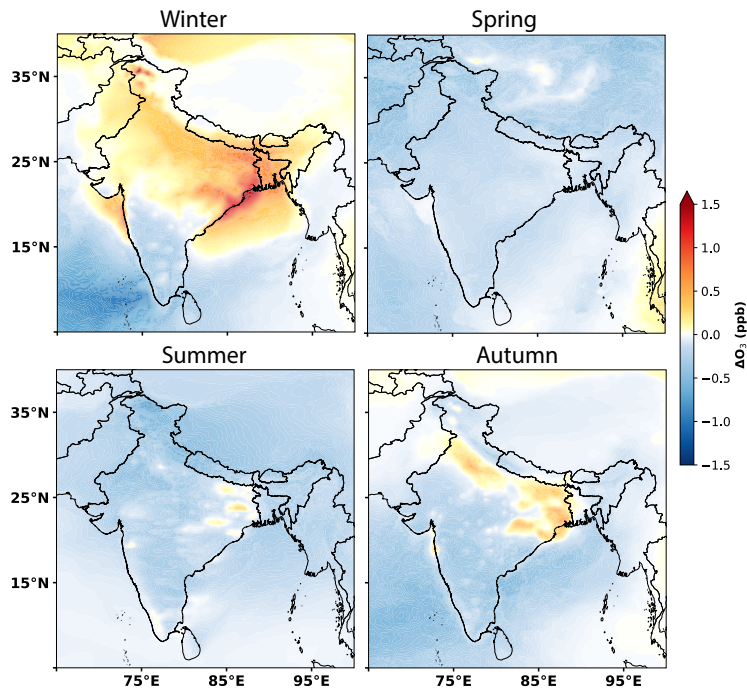


Fig. 10 Spatial distribution of  $\Delta$ MDA8 O<sub>3</sub> for each season of 2018.

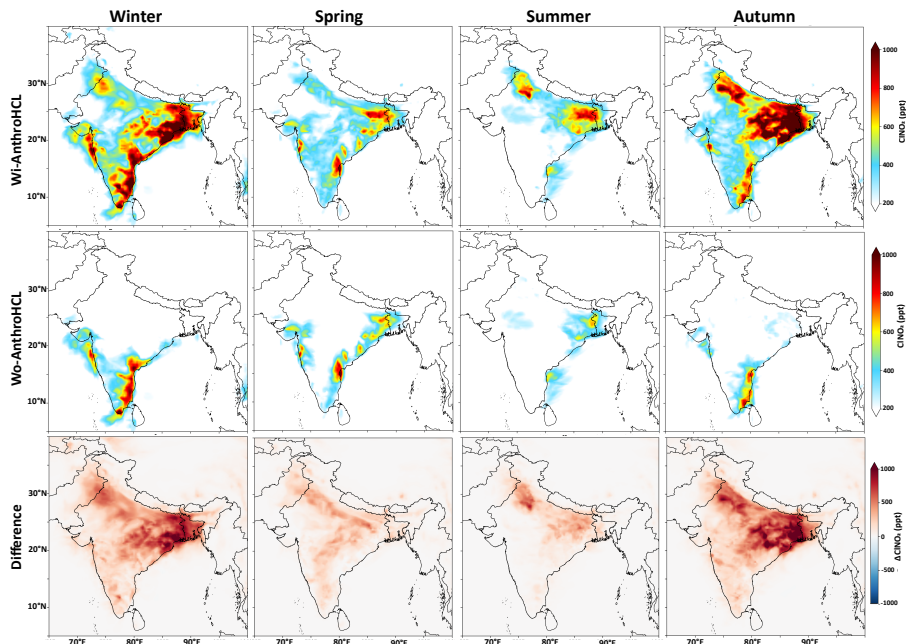


Fig. 11 Spatial distribution of ClNO<sub>2</sub> from Wi-AnthroHCL and Wo-AnthroHCL for each season along with the absolute difference between both type of simulation.



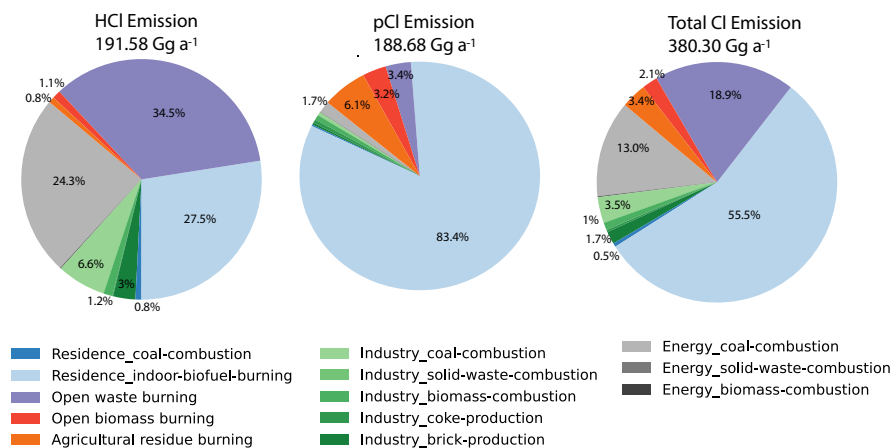


Fig. 12 Pie charts show percentage distribution of HCl, pCl<sup>-</sup>, and Total Cl (HCl + pCl<sup>-</sup>) annual emissions by source sectors.

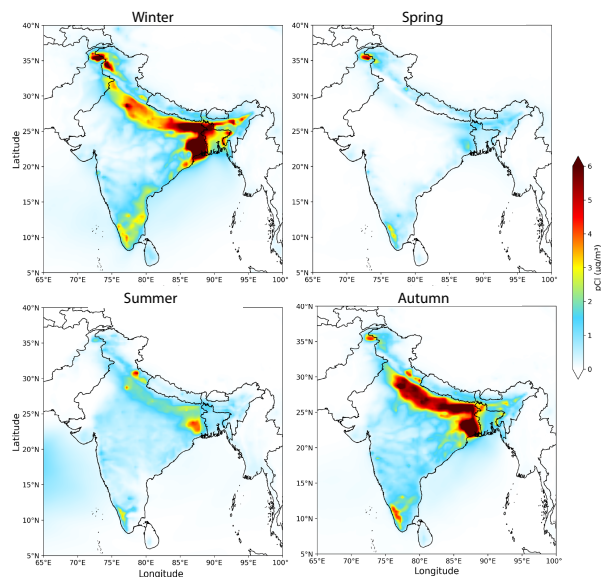
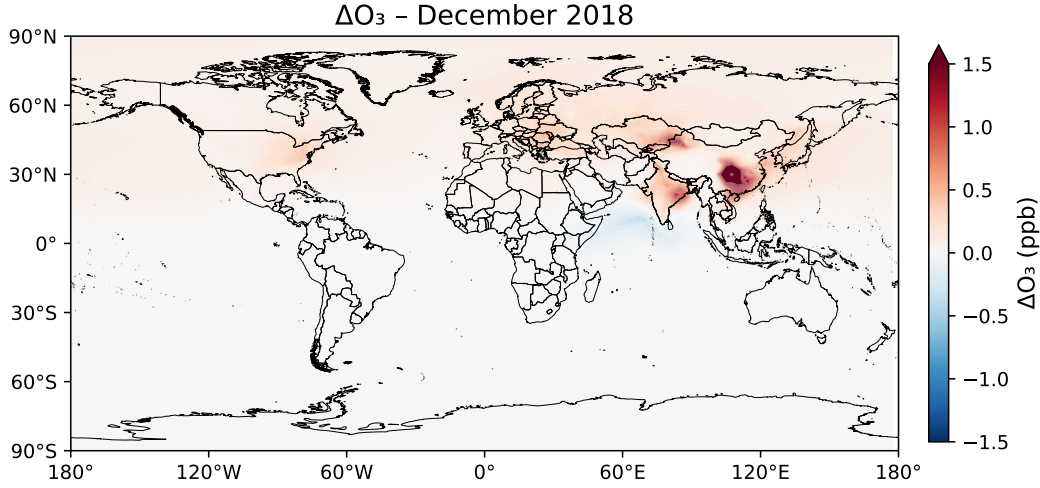


Fig. 13 Seasonal distribution of modelled pCl<sup>-</sup> concentrations ( $\mu\text{g m}^{-3}$ ) from the Wi-AnthroHCl simulation.



**Fig. 14** Global distribution of  $\Delta O_3$  for the month of December (2018) taking as a difference of Wi-AnthroHCl and Wo-AnthroHCl simulations. This figure indicate that the magnitude of tropospheric  $\Delta O_3$  over India is comparatively smaller, reflecting a weaker sensitivity to anthropogenic chlorine emissions.

**Table 1** Model performance evaluation for  $PM_{2.5}$  and  $O_3$  in Wi-AnthroHCl and Wo-AnthroHCl model simulations.

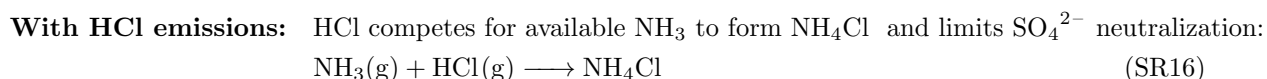
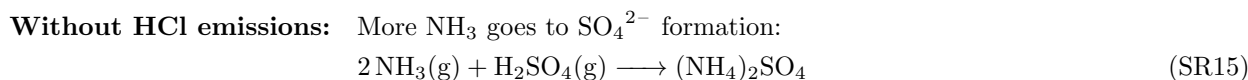
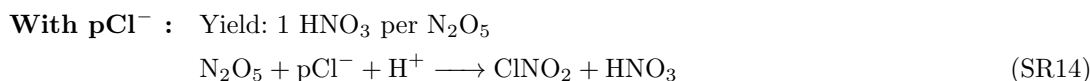
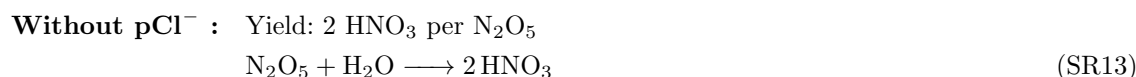
Station	Mean			NMB		$r$		IOA		
	Obs	Wi-HCl	Wo-HCl	Wi-HCl	Wo-HCl	Wi-HCl	Wo-HCl	Wi-HCl	Wo-HCl	
$PM_{2.5}$	Ahmedabad	66.56	63.96	63.32	-0.04	-0.05	0.28	0.29	0.57	0.57
	Chennai	59.04	53.51	52.49	-0.09	-0.11	0.70	0.70	0.81	0.81
	Delhi	82.16	133.66	126.91	0.63	0.54	0.57	0.56	0.62	0.64
	Kanpur	89.24	93.78	89.85	0.05	0.01	0.66	0.65	0.77	0.74
$O_3$	Ahmedabad	33.88	36.22	36.42	0.07	0.07	0.50	0.48	0.62	0.62
	Chennai	24.96	38.30	38.67	0.53	0.55	0.62	0.62	0.60	0.60
	Delhi	36.66	32.54	32.53	-0.11	-0.11	0.21	0.22	0.50	0.50
	Kanpur	24.97	55.28	55.38	1.21	1.22	0.57	0.57	0.36	0.36

**Table 2** Model performance evaluation across campaign sites for  $pCl^-$  observations.

Station	Obs Mean	Model Mean	MB	NMB	IOA
Ahmedabad	0.25	0.51	0.26	1.02	0.18
Chennai	0.83	0.54	-0.36	-0.40	0.37
Delhi	5.91	2.68	-3.27	-0.54	0.76
Kanpur	17.65	8.93	-8.72	-0.49	0.62
Munnar	0.18	0.25	0.07	0.41	0.52
Mahabaleshwar	0.09	0.14	0.05	0.56	0.22

**Table 3** Campaign details of different locations for the  $pCl^-$  and  $ClNO_2$  observations

Location	Species	Campaign Period	Reference
Ahmedabad (23.03° N, 72.58° E)	$pCl^-$	September-October 2017	[4]
Kanpur (26.45° N, 80.35° E)	$pCl^-$	January 2016	[5]
Delhi (28.61° N, 77.23° E)	$pCl^-$ , $ClNO_2$	February-March 2018, January-February 2019	[2, 3]
Chennai (13.08° N, 80.27° E)	$pCl^-$	January-February 2019	[3]
Mahabaleshwar (17.92° N, 73.65° E)	$pCl^-$	January-February 2018	This Study
Munnar (10.09° N, 77.06° E)	$pCl^-$	June-July 2021	This Study



## References

- [1] Malasani, C.R., Swain, B., Patel, A., Pulipatti, Y., Anchan, N.L., Sharma, A., Vountas, M., Liu, P., Gunthe, S.S.: Modeling of mercury deposition in india: evaluating emission inventories and anthropogenic impacts. *Environmental Science: Processes and Impacts* (2024) <https://doi.org/10.1039/d4em00324a>
- [2] Haslett, S.L., Bell, D.M., Kumar, V., Slowik, J.G., Wang, D.S., Mishra, S., Rastogi, N., Singh, A., Ganguly, D., Thornton, J., *et al.*: Nighttime no emissions strongly suppress chlorine and nitrate radical formation during the winter in delhi. *Atmospheric Chemistry and Physics* **23**(16), 9023–9036 (2023)
- [3] Gunthe, S.S., Liu, P., Panda, U., Raj, S.S., Sharma, A., Darbyshire, E., Reyes-Villegas, E., Allan, J., Chen, Y., Wang, X., *et al.*: Enhanced aerosol particle growth sustained by high continental chlorine emission in india. *Nature Geoscience* **14**(2), 77–84 (2021)
- [4] Singh, A., Satish, R.V., Rastogi, N.: Characteristics and sources of fine organic aerosol over a big semi-arid urban city of western india using hr-tof-ams. *Atmospheric Environment* **208**, 103–112 (2019)
- [5] Thampan, N.M., Joshi, B., Tripathi, S., Sueper, D., Canagaratna, M.R., Moosakutty, S.P., Satish, R., Rastogi, N.: Evolution of aerosol size and composition in the indo-gangetic plain: size-resolved analysis of high-resolution aerosol mass spectra. *ACS Earth and Space Chemistry* **3**(5), 823–832 (2019)